Numerical studies of the extended two-chain model of friction

Mario Einax, Steffen Trimper, H.-R. Höche and Michael Schulz
Fachbereich Physik, Martin–Luther–Universität
Halle,06099 Halle (Saale), Germany
(February 1, 2008)

We investigate numerically a simple microscopic model to describe wearless dry friction between atomically flat contact interfaces without thermal fluctuations ($T = 0\,K$). The analysis of the incommensurate ground state shows a breaking of analyticity when the amplitude ϵ of the Lennard-Jones interaction between the both harmonic chains increased beyond a critical value ϵ_c. By the introduction of a suitable order parameter and using a finite size scaling we could show that the breaking of analyticity is a second order phase transition. This transition is often called Aubry transition. By applying of an uniform external force F^{ex} we have determined the critical force of static friction F_c above a sliding motion occurs.

05.70.Jk, 46.30.Pa, 64.70.Rh

I. INTRODUCTION

There are several ways for studying friction phenomena. Experimental observations are very powerful to characterize the frictional behaviour and to formulate empirical friction laws, e.g., Coulomb-Amonton's laws [1], from a phenomenological point of view. Macroscopically, everybody can usually observe that during two solids are slided against each other, wear take place. But wear is not necessary for the occurrence of friction. In the last few years the technological development makes it possible to study wearless dry friction between atomically flat contact interfaces experimentally (nanotribology) [1–3]. These nano-scale experiments on systems with less complicity stimulated again the theoretical efforts to investigate friction phenomena on the base of microscopic models [4–12]. The dissipative nature of friction is a typical non-equilibrium problem. From the theoretical point of view, wearless dry friction between two atomic flat solids could be explained by using a simple driven mechanical many-body system with a lattice structure and take into account interaction forces. Thus the question arises, how the structure of such a microscopic model of friction has to look.

One of the simplest structure on the microscopic level is given by the discrete version of the well-known Frenkel-Kontorova (FK) model [13], which is in general a model of an one-dimensional harmonic chain of particles in a periodic potential. The FK model is mainly used for describing an adsorbate atom monolayer on an atomically flat clean substrate surface. Using this picture, the driven FK model, where a constant external force is applied to each particle of the chain, can also be used as a simple model structure for a wearless friction situation, which has been studied by several works [4–6]. Note, several physical phenomena such as the dislocations motion in crystals [14], commensurate-incommensurate transitions [15,16] and charge-density waves (CDW's) [17,18] could also be investigated by reducing on the FK model structure. Definitely, the simple FK model is a good starting point in order to construct more complex and realistic friction models on the atomic level. Thus, a natural extension of the FK model is the replacement of the rigid substrat (hard body) by a deformable substrat monolayer pinned on a bulk (soft body). Such a more complex model of friction was firstly introduced by Matsukawa and Fukuyama [7,8]. They considered an one-dimensional model consisting of two deformable interacting harmonic chains, where each particle of the lower chain is harmonically pinned on a rigid bulk. The static and kinetic properties of this two-chain model of friction was analysed in great details by Kawaguchi and Matsukawa [9,10]. So far, the FK model and the two-chain model are simple models of wearless friction between an atomic monolayer and a hard or soft body, respectively. For describing a more realistic friction situation, which should represent wearless friction between atomically flat bodies, it is necessary to replace the adsorbate monolayer by a substrat. For this reason, Weiss and Elmer [11,12] proposed an interesting approach, the so-called Frenkel-Kontorova-Tomlinson (FKT) model, which is an one-dimensional lattice model for a soft upper body sliding on a hard lower body. In contrast to the two-chain model, with the FKT model they extended the FK model structure in another direction by harmonically coupling of each particle of the adsorbat monolayer on an upper macroscopic sliding mass, whose position relative to the lower surface is characterized by the coordinate x_B. Note, all of these models are investigated as completely one-dimensional microscopic friction models, where the particles of the one-dimensional chain can only move parallel to the direction of the external force. Now, it is obviously clear,

how you have to extend the previous model structures in order to write down a more complex microscopic model system, which is necessary to describe friction phenomena as simple but also realistic as possible. For that purpose we introduce an extended two-chain model consisting of two interacting harmonic atomic chains embedded in a two-dimensional space, where each particle of the upper or lower chain is harmonically pinned on an upper or a lower rigid bulk, respectively. This model describes two soft bodies with an one-dimensional contact interface, which can carry out a genuine two-dimensional sliding motion against each other. In our studies we consider the extended two chain model as a simple relaxation model by taking energy dissipation via a phenomenological damping term in the mechanical equation of motion into account. Hence, all model, where the energy dissipation is modeled by hand through an explicit damping term, cannot explain the origin of friction in complex physical systems refering to the sliding state. Well, that is also not the aim of our investigations, because with our approach we want to establish the typical macroscopic friction situation (tension experiment) on a microscopic level. Nevertheless, the introduced model structure can be used to discuss the mechanism of the occurrence of static friction, which is one characteristic feature of dry friction, based on an energy concept. The hope is that the properties of the ground state - defined as the minimal potential energy state of the mechanical model system in absence of an external force - describe completely the static friction behaviour as function of the interaction between the two deformable chains. In general the ground state structure can exhibit two situations as a driven force increased from zero. On the one hand, a zero static friction arises exactly then if the maximum static friction force vanished, i.e., the model system is frictionless. On the other hand, a finite static frition corresponds always with the existence of a finite maximum static friction force, which is the maximum potential energy state of the system above which a sliding state appears. In other words, if we evolve the particle configuration from their ground state configuration, then the maximum static friction force is defined by the largest depinning force, which is equivalent to the smallest driven force above which no stable stationary state exists.

For the analysis of static properties of the extended two chain model we follow the philosophy of Aubry by using strangely enough an incommensurate ground state structure, which has the only purpose to introduce a special kind of mathematical functions called as hull-functions. On the basis of the specific hull-function concept for the visualisation of the ground state structure of the discrete FK-model in the incommensurate case Aubry [19,20] has been shown that a new type of phase transition (called as breaking of analyticity) occurs when the amplitude of the periodic potential increased beyond a critical value. That means, below a critical amplitude the hull-functions have a continuous (analytic) structure whereas above a critical amplitude the hull-functions are discrete (non analytic). In our numerical investigations of the hull-functions of the extended two chain model we have also found the transition by breaking of analyticity (Aubry transition). In order to distinguish, whether the Aubry transition is really about a second order phase transition, we have specifically studied this type of phase transition like Coppersmith and Fisher (but which have been investigate the behaviour near the maximum static friction force [17,18]) from the viewpoint of critical phenomena. For that purpose we have introduced a suitable order parameter, which shows the typical critical behaviour for second order phase transitions and critical exponents can be calculated via scaling arguments.

Here, it should mentioned, that from the physical intuition a finite maximum static friction as function of the interaction strength ϵ has to exist in all previous introduced models equal whether one choose a commensurate or an incommensurate ground state structure. The main differences are the following. In the commensurate case the static friction is always larger than zero for any $\epsilon > 0$. By way of contrast, in the incommensurate case whether the static friction is equal or unequal zero depends strongly on ϵ below or above a critical value ϵ_c due to the preculiar breaking of analyticity. Hence the commensurate and the incommensurate ground state structure reveals two types of physical system classes characterizing by different critical behaviour in the sliding state near the threshold force F_c. The first class is given by model systems with a commensurate ground state structurce. Effectively, commensurate models are characterized by finitely many internal degrees of freedom, which lead to trivial critical exponents in the sliding state for the velocity-force characteristic near the threshold F_c. An incommensurate ground state structure is equivalent to a second class of models with infintely many internal degrees of freedom. Well, both model classes emphasize the fact that the nature of static and kinetic friction is deeply rooted with internal degrees of freedom generated by a complex atomic interaction behaviour, which is the key for unterstanding dissipation in general. Commensurate model have one main disadvantage, because an uniquely visualisation concept for the ground state structure like the hull-function for the incommensurate case is missing. Moreover, commensurate models exist always in a pinned ground state structure, that means, models imply static friction for any value of the amplitude of the interaction strength larger then zero intrinsicly. Therefore, for understanding the physical fundamental mechanism of the arising of static friction it seems to be most interesting to study incommensurate models, because the ground state shows two different incommensurate phases related to amazing properties. That means, an unpinned incommensurate phase corresponds to zero static friction whereas the pinned incommensurate phase is equivalent to a finite static friction.

In the present paper we introduce the extended two chain model and the numerical calculation methods. The detailed investigations of the static properties, especially the ground state structure of the extended two chain model are discussed by defining an order parameter and proposing scaling relations.

II. THE MODEL SYSTEM

Following Matsukawa and Fukuyama [7,8], we introduce the extended two-chain model, which is a two-dimensional microscopic lattice model system describing wearless dry friction between two atomically flat solids. Therefore, we consider two deformable atomic chains, so called an upper and a lower chain. The atoms in each chain are classical point particles and are able to realize a two-dimensional movement. We assumed a harmonic particle interaction in each chain. The interaction between the two chains is of the Lennard-Jones type. Moreover, both chains are coupled harmonically on an upper or a lower substrat respectively. Like Ref. [7] the effects of energy dissipation in the upper and lower chain are phenomenologically approached to be proportional to the difference between the velocity of the i-th particle and that of the center of gravity. The external force $\underline{F}^{ex} = (F^{ex}, 0)$ acts on the upper chain in x direction without y component. In order to simplify the situation, we consider overdamped motion. The equations of motion for the particles in the upper and the lower chain are given for each direction as follows (see also FIG. 1)

$$m_a\gamma_a\left(\dot{x}_i^a - \langle\dot{x}_i^a\rangle\right) = k_a^x\left[x_{i-1}^a + x_{i+1}^a - 2x_i^a\right] - k_{sub}^{a_x}\left[x_i^a - ic_a\right] + \sum_{j=1}^{N_b} F_{int}^x\left(x_i^a - x_j^b\right) + F^{ex} \tag{1}$$

$$m_a\gamma_a\left(\dot{y}_i^a - \langle\dot{y}_i^a\rangle\right) = k_a^y\left[y_{i-1}^a + y_{i+1}^a - 2y_i^a\right] - k_{sub}^{a_y}\left[y_i^a - (b_b + L_0)\right] + \sum_{j=1}^{N_b} F_{int}^y\left(y_i^a - y_j^b\right) \tag{2}$$

$$m_b\gamma_b\left(\dot{x}_i^b - \langle\dot{x}_i^b\rangle\right) = k_b^x\left[x_{i-1}^b + x_{i+1}^b - 2x_i^b\right] - k_{sub}^{b_x}\left[x_i^b - ic_b\right] + \sum_{j=1}^{N_a} F_{int}^x\left(x_i^b - x_j^a\right) \tag{3}$$

$$m_b\gamma_b\left(\dot{y}_i^b - \langle\dot{y}_i^b\rangle\right) = k_b^y\left[y_{i-1}^b + y_{i+1}^b - 2y_i^b\right] - k_{sub}^{b_y}\left[y_i^b - b_b\right] + \sum_{j=1}^{N_a} F_{int}^y\left(y_i^b - y_j^a\right), \tag{4}$$

where $\underline{r}_i^a = (x_i^a, y_i^a)$ and $\underline{r}_i^b = (x_i^b, y_i^b)$ are the immediately position vectors of the i-th particle in the upper and lower chain. Furthermore, N_a (N_b), m_a (m_b) is the particle number and the particle mass, γ_a (γ_b) denotes the friction coefficient and c_a (c_b) is the mean atomic spacing in x-direction of the upper (lower) chain. It should be mentioned, that the particle mass and the friction coefficient are for all particles in each chain the same. For a compact representation one can introduce the chain index $I = (a, b)$ relating to the upper and lower chain. The velocity of the center of gravity is given by the average $\left\langle\dot{X}_i^I\right\rangle = \frac{1}{N_I}\sum_{i=1}^{N_I}\dot{X}_i^I$, where $\dot{X}_i^I$ stands for $\dot{x}_i^I$ and $\dot{y}_i^I$ respectively. k_I^x and k_I^y are the strength of the harmonic interaction force in the chains for the x and y direction. The strenght of the coupling of each chain on an upper and a lower substrat is represented by $k_{sub}^{I_x}$ and $k_{sub}^{I_y}$, which determine the rigiditiy of the chains. A further system parameter is the substrat-substrat distance $L = b_a + b_b + L_0$, where b_a (b_b) is the mean atomic spacings in y-direction between the upper (lower) chain and upper (lower) substrat. L_0 denotes the distance between the two harmonical chains and is a function of their interaction strength. The interaction force between the upper and lower chain, projected on the x and y axes, can be written as

$$\sum_{j=1}^{N_J} F_{int}^x\left(x_i^I - x_j^J\right) = \sum_{j=1}^{N_J} F(r_{ij})\,\frac{\left(x_i^I - x_j^J\right)}{r_{ij}} \tag{5}$$

$$\sum_{j=1}^{N_J} F_{int}^y\left(y_i^I - y_j^J\right) = \sum_{j=1}^{N_J} F(r_{ij})\,\frac{\left(y_i^I - y_j^J\right)}{r_{ij}} \tag{6}$$

with the chain indices $I = (a, b)$, $J = (b, a)$ and the distance $r_{ij} = \left|\underline{r}_i^a - \underline{r}_j^b\right| \equiv \sqrt{(x_i^b - x_j^a)^2 + (y_i^b - y_j^a)^2}$ relating to the i-th atom of the upper (a) and the j-th atom of the lower (b) chain. $F(r_{ij})$ can be expressed by the potential $V(r_{ij})$ through $F(r_{ij}) = -\frac{\partial V(r_{ij})}{\partial r_{ij}}$. As interaction potential we choose specifically the Lennard-Jones potential

$$V(r_{ij}) = 4\epsilon\left[\left(\frac{\sigma}{r_{ij}}\right)^{12} - \left(\frac{\sigma}{r_{ij}}\right)^{6}\right] \tag{7}$$

representing the character of the friction due to the intermolecular forces in the best way. Here ϵ is the strength of the interaction and σ is a characteristic length parameter, which parameterized the minimum of the potential $V^{min} = V(r_{ij})|_{r_{ij}=r_0}$ via the distance from equilibrium $r_0 = \sigma\,2^{1/6}$.

III. NUMERICAL METHOD

For solving the two-dimensional extended two-chain lattice model we choose periodic boundary conditions in both chains

$$x_i^I = x_{i+N_I}^I - L_I \tag{8}$$

$$y_i^I = y_{i+N_I}^I \tag{9}$$

with the chain index $I = a, b$ and the chain lengths $L_I = N_I c_I$. This implies that the system size of the upper and lower chain are the same $L \equiv N_a c_a = N_b c_b$. Hence, the ratio or the misfit of the two lattice constants could be expressed by the particle numbers

$$\alpha = \frac{c_a}{c_b} = \frac{N_b}{N_a}\,. \tag{10}$$

This means, that the ratio α of the two lattice constants is always a rational number in the numerical realisation. Using the concept of the hull-function, which was introduced by Aubry and coworkers [19,20] for describing the ground state of the underlying model system, we need an irrational ratio α between c_a and c_b. If we have a rational α, i.e., in the most commensurable case $\alpha = 1$, we cannot apply the concept of the hull-function. Because the whole ground state configuration of each chain, consisted of N_I particle positions, would be represented by one value of the argument of the hull function and hence the hull-function plot lose his mathematical power of proposition. For this reason, it is necessary to investigate an incommensurate ground state structure relating to the ratio α of the two lattice constants. Unfortunately, in the numerical calculation we could only approximate an irrational number through optimal rational ratios of two natural numbers using a finite continued-fraction expansion up to a certain order [18,19]

$$\alpha = a_0 + \cfrac{1}{a_1 + \cfrac{1}{a_2 + \cfrac{1}{\ldots + \cfrac{1}{a_{n-1} + \cfrac{1}{a_n}}}}} \tag{11}$$

Following the literature, we choose the simplest continued-fraction expansion with $a_0 = 1$ and $a_1 = a_2 = \cdots = a_n = 1$, so that α could be expressed by the ratios of the Fibonacci numbers $F_{n+1} = F_n + F_{n-1}$, where $n = 1, 2, 3, \cdots$ as well as $F_0 = 1$ and $F_1 = 1$. Hence,

$$\alpha = \frac{F_{n+2}}{F_{n+1}} = \frac{3}{2}, \frac{5}{3}, \frac{8}{5}, \frac{13}{8}, \frac{21}{13}, \frac{34}{21}, \frac{55}{34}, \frac{89}{55}, \frac{144}{89}, \frac{233}{144}, \frac{377}{233}, \frac{610}{377}, \frac{987}{610}, \frac{1597}{987}, \cdots \tag{12}$$

and the irrational limit $\alpha \equiv \lim_{n\to\infty} \frac{F_{n+2}}{F_{n+1}} = \frac{1}{2}\left(\sqrt{5}+1\right)$ of the approximation series (12) is the inverse of the so-called *golden mean*. From the point of number theory [19] , this is the most incommensurable case of the underlying model system, which could be emulated in a systematical way. In our studies we set the lattice constant of the lower chain equal one ($c_b = 1$). Accordingly, the upper mean lattice spacing c_a is equal α and we calculated with the system sizes

$$c_a = \frac{N_b}{N_a} = \frac{89}{55}, \frac{233}{144}, \frac{377}{233}, \frac{610}{377}, \frac{1597}{987}\,. \tag{13}$$

It should be mentioned, that not all ratios oft the approximants are "good" irrational number approximations in the same manner because for certain particle number ratios there exist some artifacts in the hull function.
For the numerical calculation of the equations of motion we used a fourth-order Runge-Kutta algorithm with an adaptive stepsize control. In order to discuss the essential features of the present model we restrict the wide range of model parameters by setting $m_I = 1$, $\gamma_I = 1$, $k_I^x = k_I^y = 1$, $k_{sub}^{I_x} = k_{sub}^{I_y} = 1$ and $\sigma = 1$. As initial conditions we assumed at $t = 0$ a particle configuration in the x-y-plane, where the N_a and N_b chain particles are arranged at regular lattice sites periodically. Besides, the distance L_0 is set to an arbitrary initial value, i.e. $L_0 = 1$. For calculating the stable stationary states we used the same criterion like Kawaguchi and Matsukawa [10]. That means, we used a velocitiy condition

$$\sqrt{\frac{\left(\sum_{i=1}^{N_a}(\dot{r}_i^a)^2 + \sum_{j=1}^{N_b}(\dot{r}_j^b)^2\right)}{(N_a+N_b)}} < 10^{-5} \tag{14}$$

for stopping the Runge-Kutta calculation. Hence, the system could be considered to be in a static state. The next step consists in the check up of the total sum of the coupling forces in the (a)-chain and (b)-chain in x-direction

$$F_{sub}^{a_x} = \sum_{i=1}^{N_a} k_{sub}^{a_x} \big[\, x_i^a - i c_a \, \big] \quad , \quad F_{sub}^{b_x} = \sum_{j=1}^{N_b} k_{sub}^{b_x} \big[\, x_j^b - j c_b \, \big] \tag{15}$$

and y-direction

$$F_{sub}^{a_y} = \sum_{i=1}^{N_a} k_{sub}^{a_y} \big[\, y_i^a - (b_b + L_0) \, \big] \quad , \quad F_{sub}^{b_y} = \sum_{j=1}^{N_b} k_{sub}^{b_y} \big[\, y_j^b - b_b \, \big] \tag{16}$$

respectively. In absence of a driven force ($F^{ex} = 0$) it is sufficient to consider only the value of the total sum of the coupling forces (16) in y-direction, because for $t = 0$, after the Runge-Kutta steps and in the final state the x-direction forces (15) are equal to zero. The regular periodical arrangement of the particles for the initial time $t = 0$ leads to $F_{sub}^{a_y} = F_{sub}^{b_y} = 0$. After the relaxation in the final stationary state relating to the velocity condition (14) the total sum of coupling forces (16) must always be zero, which is in general not true for an arbitrary chosen initial value L_0. Accordingly, during the numerical calculation every final stable state in respect to L_0 must be proofed and if necessary L_0 must be changed like $\text{Ł}_0 = L_0 \pm \delta L_0$. Then the chains relax again and the procedure would be repeated until the system reached a final stationary state, which fulfil the condititon $F_{sub}^{a_y} = F_{sub}^{b_y} < 5 \cdot 10^{-5}$ ($\simeq 0$). In this way we could find numerically the stationary configuration of the extended two-chain model and for $F^{ex} = 0$ one can assumed that this is approximately the ground state, defined as having an energy which cannot be lowered by moving of some system particles. The properties of the ground state could be analysed by changing the interaction strength ϵ, which corresponds to set the correct $L_0 = L_0(\epsilon)$ numerically.
In the presence of an external force $F^{ex} > 0$ acting in x-direction one must slightly change the numerical calculation procedure. Instead of $F_{sub}^{a_x} = F_{sub}^{b_x} = 0$ the x-direction forces (15) have for $t = 0$ the values $F_{sub}^{a_x} = F^{ex}$ and $F_{sub}^{b_x} = 0$ respectively. After each Runge-Kutta step we have to guarantee that the control parameters (15) have again these values. Hence, we are able to evolve the model system from the ground state into the last possible static solution by continuously increasing of the applied external force. In this sense we could numerically define the threshold, where no longer a static solution of the underlying system exist. This threshold $F^{ex} = F_c$ is the critical force of static friction, which is also called maximum static frictional force. Below $F^{ex} < F_c$ the chains are in a steady state, such that the afterwards space-time averaged velocity $v \equiv \langle \dot{x}_i^a \rangle_{i,t} = 0$. Above $F^{ex} > F_c$ the upper chain, which is after an initial transient decay in a steady sliding state, slides with a constant velocity v. Note, in an easy way one can investigate the present model in a gravitational field via the constraints (16).

IV. NUMERICAL RESULTS

A. Ground state

First, we investigate the stationary states of the extended two-chain model in the absence of an external force, i.e., $F^{ex} = 0$. The stationary states are given by the solution of equation system (1-4) with vanishing right-hand side

$$0 = m_a \gamma_a \, (\, \dot{\underline{r}}_i^a - \langle \dot{\underline{r}}_i^a \rangle \,) = m_b \gamma_b \, \big(\, \dot{\underline{r}}_i^b - \big\langle \dot{\underline{r}}_i^b \big\rangle \, \big) \tag{17}$$

with consideration of the conditions (15) and (16), where $F_{sub}^{a_x} = F_{sub}^{a_y} = F_{sub}^{b_x} = F_{sub}^{b_x} = 0$. Hence, the ground state of the extended two chain model is the stationary particle configuration having the minimal potential energy for $F^{ex} = 0$. The knowledge of the ground state determine a physical system, such as the static friction, completely.

1. The hull-function

Similarly to the FK model [19] or FKT model [11], the lattice structure of the particle positions in the incommensurate ground state can be uniformly described by a hull-function. For examining the lattice structure of the present two-dimensional extended two-chain model, it is necessary to introduce four hull-function due to two degrees of freedom of the particles in each chain. The two hull-functions h_a and h_c of the upper chain are defined as

$$x_i^a = i\,c_a + \phi + h_a(i\,c_a + \phi) \tag{18}$$
$$y_i^a = b_b + L_0 + \phi' + h_c(i\,c_a + \phi') \tag{19}$$

and the two hull-function h_b and h_c of the lower chain are given by

$$x_i^b = i\,c_b + \psi + h_b(i\,c_b + \psi) \tag{20}$$
$$y_i^b = b_b + \psi' + h_d(i\,c_b + \psi')\ , \tag{21}$$

where ϕ, ϕ', ψ and ψ' are constant phases. For our investigations, it is conviencent to set $\phi = \phi' = \psi = \psi' = 0$. The hull-functions are periodic and even, which can usually be expressed by

$$h_a(z + c_b) = h_a(z) = -h_a(-z), \quad h_c(z + c_b) = h_c(z) = -h_c(-z) \tag{22}$$
$$h_b(z + c_a) = h_b(z) = -h_b(-z), \quad h_d(z + c_a) = h_d(z) = -h_d(-z)\,. \tag{23}$$

The argument z of h_a and h_c is defined in the range from 0 to c_b, whereas of h_c and h_d it is given from 0 to c_a. Note, the visualisation concept of the hull-function makes it necessary that the argument of the just defined hull-functions h_a, h_c or h_b, h_d must be the same, respectively. Because, the displacements in x- resp. y-direction of all particle in each chain can be assigned to different values of the argument z due to the irrational ratio α of the mean lattice spacing c_a and c_b.

First, we have numerically calculated the ground state of the extended two-chain model for a fixed ratio $\alpha = N_b/N_a$ of the particle numbers given by $N_a = 233$ and $N_b = 377$. Several investigations of the FK model [20], FKT model [11] such as the two-chain model [10] showed, that the ground state strongly depends on the interaction strength ϵ. Therefore, we started the computation for different values of ϵ in the wide range from 0.05 to 0.4. For small values of ϵ up to a certain value ϵ_c we get the result that the periodic hull-functions h_a, h_b, h_c and h_d are analytic, i.e, smooth and continuous. This behaviour is illustrated in Fig. 2, where the interaction strength has the value $\epsilon = 0.22$. Furthermore, the stationary state for $\epsilon = 0.22$ is characterized by the distance $L_0 = 0.986273$ between the upper and lower chain. Figure 3 shows another numerical calculation of the hull-functions for the interaction strength $\epsilon = 0.33$ with the corresponding distance $L_0 = 0.959584$. We can see that the hull-functions in Fig. 3 are discrete, which means that they are no longer analytic. This discrete structure is related to jumps, which occur at certain points of the argument z of the hull-functions. Now, the comparison of Fig. 2 with Fig. 3 shows the phenomenon of breaking of analyticity, which is due to two significant aspects of the hull-functions h_a, h_b, h_c and h_d for the interaction strength $\epsilon < \epsilon_c$ and $\epsilon > \epsilon_c$, which defined a certain transition value ϵ_c above the hull-functions are no longer analytic. For a detailed analysis of the threshold ϵ_c we introduced a suitable order parameter in the following part.

Well, Aubry has shown [20] that the breaking of analyticity of the incommensurate ground state of the FK model is characterized by the existence of a largest central gap at the half of the period of the hull-function. Whereas the situation in the two-chain model of Matsukawa and Fukuyama [10] is quite different for several elastic parameters and three simple cases are observed: both hull-functions h_a and h_b have a largest gap at the half of the period (FK limes), whether h_a or h_b has only a largest central gap and finally both hull-functions do not have a largest central gap but two symmetrical gaps with the same size refering to the half of the period. In Fig. 3 we can also observe that no largest central gap for all hull-functions of the extended two-chain model exists. Furthermore, the hull-functions show also two symmetrical gaps of the same size refering to the half of the period of the hull-function in the whole analysed parameter range. Up to now we have only investigated the ground state structure for a fixed system size ($N_a = 233$ and $N_b = 377$) and a certain range of interaction strength ϵ. Now, we vary the system size of the underlying model which corresponds the different approximation orders of the irrational number through a rational ratio of the particle numbers. Here, we calculated especially the ground state structure for the ratios $\alpha = 89/55$, $233/144$, $610/377$, and $1597/987$ in the same range of the interaction strength ϵ like above. In particular, we proofed whether there occurs an anormalous behaviour in the structure of the hull-functions for certain values of ϵ due to the using of a rational ratio instead of an irrational number in the numerical computation. Indeed, Fig. 4 shows such a anormalous behaviour of the hull-functions for $\epsilon = 0.33$ and for the particle numbers $N_a = 377$ and 610. In the comparison with Fig. 3 we can recognize that the even particle number $N_b = 610$ generates a wrong particle position at the half of the period $x = 0.5$ of h_b in Fig. 4 due to the periodical boundary condition. Consequently, in term of a suitable rational particle ratio Fig. 3 shows the right picture of the hull-functions for $\epsilon = 0.33$, whereas Fig. 4 shows some artifacts in the hull-function structure for the same interaction strength $\epsilon = 0.33$ as a result of bad choice $N_a = 377$ and $N_b = 610$ of the system size for the interaction strength $\epsilon = 0.33$. Beyond it, there appear much more artifacts in the hull-function structure different ranges of ϵ als consequence of a bad choice for the particle number ratios. For $N_a = 144$ and $N_b = 233$ the occurence of such artifacts destroyed the order parameter analysis of the transition area. Kawaguchi and Matsukawa interpreted in [10] these artifacts, which also occur in the two-chain model for certain values of the interchain strength and $N_a = 144$, $N_b = 233$, as information of the appearance of a new gap structure at the elastic parametes K_b. This

interpretation is wrong, because, if they calculated the model system with the same interaction strength for different particle numbers these artifacts will be vanished. The appearence of artifacts in the hull-function for the ground state defines the range of validity of the hull-function concept for several ϵ in the numerical calculation, which makes it necessary to proof the hull-function structure for the same ϵ for several system size. Relating to stationary state which is given by Eq.(17), Fig. 5 shows the distance L_0 between the upper and the lower chain as a function of the strength ϵ of the interaction force, which was calculated for the particle numbers $N_a = 233$ and $N_b = 377$. The plot in Fig. 5(a) shows the computation of L_0 for ϵ in range from 0.05 to 0.45 and Fig.5(b) shows L_0 in the transition area. Note, the distance L_0 is remarkably insensitiv to the system size. For the system sizes $\alpha = 377/233$, 610/377, and 1597/987 we found a deviation for $L_0 = L_0(\alpha)$ smaller than 10^{-5}. In the occurence of local artifacts in the hull-functions for certain particle numbers and certain interaction strength the deviation for $L_0(\alpha)$ lies in the order 10^{-4}. Note, that in the ground state above the transition point ϵ_c also many local rearrangements take place which can be identified as first order phase transitions.

2. The order parameter

Now, we analyse the transition of breaking the analyticity near the threshold ϵ_c in terms of second order phase transition. For this it is convenient to introduce an order parameter, which is an indicator for the occurence of a phase transition at a critical point. The order parameter distinguishs both phases which are involved in the phase transition, because it is defined to be zero in one phase. Refering to the transition of breaking of analyticity the order parameter is defined in the discrete phase, which measures the discrete jumps in the hull-functions. Therefore the order parameter is in the continuous phase for $\epsilon < \epsilon_c$ equal to zero and in the discrete phase above ϵ_c unlike zero. Here, we use the definition

$$OP_m = \frac{\int_0^1 \left| \frac{\partial^m f(z)}{\partial z^m} \right|^2 dz}{\delta(0)} \quad . \tag{24}$$

Here, $\delta(0)$ behaves like $\delta(0) \sim \Delta z^{-1}|_{\Delta z \to 0}$. If the hull-function is smooth in the interval $[0,1]$, the integral becomes finite and the order parameter vanished due to the prefactor $\delta(0)^{-1}$. On the other hand, if $f(z)$ has a discrete step at z_0, we obtain $\partial_z f(z) \sim \delta(z - z_0)$ and therefore $\int_0^1 [\partial_z f(z)]^2 dz \sim \int_0^1 \delta(z - z_0)^2 dz \sim \delta(0) \int_0^1 \delta(z - z_0) \sim \delta(0)$, i.e. the order parameter becomes finite. Due to the finite system size, which devides the region of integration in equidistant subintervals $\Delta z = 1/N_a$ ($\Delta z = 1/N_b$) for the upper (lower) chain, the integral in Eq.(24) reduced to a sum over the particle numbers. Therefore, we have intrinsic discontinuities in the numerical computation, because the hull-functions are given by a discrete set of points at Δz at all, which define the systematical error of the calculation. In order to smeared out the systematical intrinsic discontinuities, we choose for our numerical investigation OP_4 as order parameter. Hence, we get the following expression

$$OP \equiv OP_4 = \frac{\int_0^1 \left| \frac{\partial^4 f(z)}{\partial z^4} \right|^2 dz}{\delta(0)} \equiv \frac{1}{(\Delta z)^6} \sum_{k=2}^{\substack{(N_b-2) \\ N_a-2}} \left(|\, f_{k+2} - 4\, f_{k+1} + 6\, f_k - 4 f_{k-1} + f_{k-2}\, | \right)^2 \tag{25}$$

It should mentioned, that OP shows necessary for all hull-functions h_a, h_c, h_c and h_d the same qualitativ behaviour. Therefore, in order to show all basic features of the phase transition (transition of breaking of analyticity) it is enough to calculate OP (via Eq.(25)) only for the hull-function $h_a = h_a(z)$.

3. The scaling behaviour

Next we have calculated the order parameter given by Eq.(25) for different system sizes $\alpha = 89/55$, 233/377, 610/377 and 1597/987. Figure 6(a) shows the order parameter as function of the interaction strength ϵ in the transition region. We clearly see that the order parameter OP is changed from zero below a certain critical threshold ϵ_c to a value unlike zero above ϵ_c for all particle number ratios. This is a certain hint that the transition of breaking of analyticity is a second order phase transition. Using a finite-size scaling [23,24] for the data in Fig. 6(a) given by the scaling function

$$OP(\epsilon - \epsilon_c, L) = L^{\frac{\beta}{\delta}} OP\left(L^{\frac{1}{\delta}} (\epsilon - \epsilon_c) \right) \tag{26}$$

we find that the order parameter OP exhibits a scaling behaviour in the transition region shown in Fig. 6(b). That means, all curves of Fig. 6(a) could mastered on one resulting curve (Fig. 6(b)). The system size L is determined by the particle numbers 55, 233, 377 and 987. In the transition region, which can be characterized by the reduced interaction strength $t = (\epsilon - \epsilon_c)/\epsilon_c$, we find that the data of Fig. 6(b) are consistent with the following power law for $\epsilon > \epsilon_c$

$$OP(\epsilon - \epsilon_c) \sim L^{\frac{\beta}{\delta}} \, (\epsilon - \epsilon_c)^{\beta} \tag{27}$$

with the critical exponents $\beta = 0.239 \pm 0.05$, $\delta = 0.687 \pm 0.05$ defining the ratio $\mu = \beta/\delta \approx 0.347 \pm 0.05$. Due to the finite-size scaling we obtain for the threshold interaction strength of the transition of breaking of analyticity the critical value $\epsilon_c = 0.25575 \pm 0.001$.

B. The static friction

In the following we want to calculate the maximum static friction force F_c of the extended two-chain model refering to a pinning structure which is given in the incommensurate case for $\epsilon > \epsilon_c$. It is clear that in the presence of an applied forces $F^{ex} > 0$ ground states are no longer defined. From the physical intuition, we hope that one can adiabatically evolve the underlying model system from the ground state by increasing F^{ex} from zero, because the threshold force F_c is the largest depinning force F^{ex} above no a longer stationary state exist, i.e., Eq.(17) is no longer valid. Like Ref. [10] the static friction is given by

$$F_R = -\sum_{i=1}^{N_a} \sum_{j=1}^{N_b} \left\langle \, F_{int} \left(x_i^a - x_j^b \right) \right\rangle_t \equiv N_a \left\langle \, F^{ex} \, \right\rangle_t \tag{28}$$

which can be obtained from the equation of motion (1)-(4) by summing over i and averaging with respect to t. It should remarked, that Eq.(28) is also valid for the calculation of the kinetic friction in a sliding state, i.e., for $F^{ex} > F_c$. For the determination of the threshold force F_c, we choose especially the interaction force $\epsilon = 0.33$ and the system size $N_a = 233$ and $N_b = 377$. Note, the numerical calculations of F_c for the extended two-chain model are very hard and the computation time is very large. In a first calculation, we find that the maximum static friction force has approximately the value $F_c \approx 0.4$ but the numerical deviation is very large. Therefore, it takes much more efforts in order to calculate the accurate value of the threshold force.

V. CONCLUSIONS

We have investigated the ground state for a two-dimensional extended two-chain model with an incommensurate lattice structure. We have found that the structure of the hull-functions depends strongly on the strength ϵ of the interaction between the upper and the lower body. It was numerically observed the breaking of analyticity in the ground state for the critical value $\epsilon_c = 0.25575$. Furthermore, it was shown that this type of phase transition could be uniform described by an order parameter. This order parameter representation allows a systematic analysis of the critical behaviour for $\epsilon > \epsilon_c$ due to the calculation of the critical exponents. Consequently, the peculiar breaking of analyticity shows all features of a second order phase transition.

A second interesting result of the ground state structure occurs in associtation with the numerical computation for different interaction strengths as function of the rational system sizes. It has been shown that artifacts in the hull-functions structure appear for certain rational particle numbers of a fixed interaction strength ϵ. This fact pointed out that the correct ground state structure depends strongly on the choose of sufficient rational ratio of the particle numbers as a irrational number approximation for a certain range of the interaction force.

Concerning the static properties of the extended two-chain model in the presence of an applied forces $F^{ex} > 0$ we have calculated the maximum static friction force F_c.

Finally, it should remarked, that the extended two-chain model is a simple model structure , which established the macroscopic dry friction situation on the microscopic level between atomically flat surfaces by using a simple driven mechanical many-body system. It is convenient to define the model as simple as possible in order to dicuss some basic features like the ground state structure or the maximum static friction behaviour. Therefore we took in our investigation a simple relaxation dynamic into account and neglected thermal fluctuation ($T = 0\,K$). Surely, such kind of microscopic models could be always extended by additional thermal fluctuations representing by stochastical forces which leads to creep in the presence of applied forces. Note, the vality of the underlying model system is given

by the assumption of simple harmonic particle interaction. It is clear that this assumption in many real systems where large distortions occur.

Note, there are one possible and very interesting extention of the extended two-chain model by the introduction of quenched randomess which corresponds surface impurities. It is an open question, whether randomess destroy the frictionless state in the incommensurate case for $\epsilon < \epsilon_c$ in the extended two-chain model like in the FK-model [7,8]. Well, it is an interesting question, whether randomess, which exists in any real system, leads in general to a finite maximum static friction force for any interaction strength ϵ. Refering to the compare whith experiments, another natural extention of the present model is to proceed to a three-dimensional system, which is able to describe wearless dry friction between two atomically flat plans pinning in each case on a substrat and embeding in a three-dimensional space.

In later works we want to investigate the threshold behaviour near F_c especially for $F^{ex} > F_c$. It should be proofed whether the velocity-force characteristics shows a critical behaviour or not. Well, for a complete understanding of the behaviour near the threshold F_c a renormalization group calculation is needed, but surely very complicated for a deterministic mechanical system.

Note in the present paper, we have considered a simple overdamped motion. Hence, it is also interesting to discuss the influence of inertia terms (underdamped dynamic) on the behaviour near the threshold F_c and on the sliding state.

ACKNOWLEDGMENTS

This work has been supported by the Graduiertenkolleg "Defektstrukturbestimmte physikalische Eigenschaften" and the Deutsche Forschungsgemeinschaft DFG (SFB 418).

---

[1] **B.N. J. Persson** *Sliding Friction, Physical Principles and Applications* (Springer Verlag, Berlin, 1998)

[2] **C.M. Mate, G.M. McClelland, R. Erlandsson, S. Chiang** *Phys. Rev. Lett.* **59** *1942 (1987)*

[3] **E. Meyer, R. Lüthi, L. Howald, H.-J. Güntherodt**, in *Forces in Scanning Probe Methods* H.-J. Güntherodt and D. Anselmetti and E. Meyer (eds.), (Kluwer Academic Publishers, Dordrecht, 1995).

[4] **M. Hirano, K. Shinjo**, *Phys. Rev. B* **41**, *11837 (1990)*

[5] **K. Shinjo, M. Hirano**, *Surf. Sci.* **283**, *473 (1993)*

[6] **T. Strunz, F.J. Elmer**, in *Physics of sliding friction* B.N.J. Persson and E. Tosatti (eds.), (Kluwer Academic Publishers, Dordrecht, 1996).

[7] **H. Matsukawa, H. Fukuyama**, *Phys. Rev. B* **49**, *17286 (1994)*

[8] **H. Matsukawa, H. Fukuyama**, in *Physics of sliding friction* B.N.J. Persson and E. Tosatti (eds.), (Kluwer Academic Publishers, Dordrecht, 1996).

[9] **T. Kawaguchi, H. Matsukawa**, *Phys. Rev. B* **56**, *13932 (1997)*

[10] **T. Kawaguchi, H. Matsukawa**, *Phys. Rev. B* **58**, *No.23 (1998)*

[11] **M. Weiss, F.J. Elmer**, *Phys. Rev. B* **53**, *7539 (1996)*

[12] **M. Weiss, F.J. Elmer**, in *The physics of sliding friction,* B.N.J. Persson and E. Tosatti (eds.), (Kluwer Academic Publishers, Dordrecht, 1996).

[13] **J. Frenkel, T. Kontorova**, *Zh. Eksp. Teor. Fiz* **8**, *1340 (1938)*; *J. Phys. (Moscow)* **1** *137 (1939)*

[14] **F.C. Frank, J.H. van der Merve**, *Proc. Royal Soc. (London)* **A198**, *205 (1949)*

[15] **P. Bak**, *Rep. Prog. Phys.* **45**, *587 (1982)*

[16] **W. Selke**, in *Phase Transitions and Critical Phenomena* Vol. 15, C.Domb and J.L. Lebowitz (eds.)

[17] **S.N. Coppersmith**, *Phys. Rev. B* **30**, *410 (1984)*

[18] **S.N. Coppersmith, D.S. Fisher**, *Phys. Rev. A* **38**, *6338 (1988)*

[19] **S. Aubry**, in *Solitons and Condensed Matter Physics,* edited by A.R. Bishop and T. Schneider, Solid State Sciences, Vol. 8 (Springer, Berlin, 1978) p. 264

[20] **H. Peyrard, S. Aubry**, *J. Phys. C* **16**, *1593 (1983)*

[21] **I.N. Bronstein** *Teubner-Taschenbuch der Mathematik* (Teubner Verlag, Leipzig, 1996)

[22] **P. Cvitanovic**, in *From Number Theory to Physics* M. Waldschmidt, P. Moussa, J.-M. Luck, C. Itzykson (eds.), (Springer Verlag, Berlin, 1992)

[23] **D. Stauffer, A. Aharony** *Introduction to computer simulations* (VCH-Verlag, Weinheim, 1995)

[24] **K. Binder, D.W. Heermann** *Monte Carlo Simulation in Statistical Physics* (Springer Verlag, Berlin, 1997)

FIGURES

FIG. 1. A schematic picture of the two-dimensional extended two-chain model. The external force $\tilde{F}^{ex}$ is given by the applied force F^{Fex} which acts on each particle of the upper chain times the particle number N_a of the upper chain where N_a, (N_b) is the particle number of upper (lower) chain.

FIG. 2. The hull-functions of the ground state plotted for the particle numbers $N_a = 233$ and $N_b = 377$ with the interaction strength $\epsilon = 0.22$. For an uniform representation all hull-functions are renormalized by the mean lattice spacing c_b and c_a, respectively. Therefore, the substitution for the hull-function h_a and h_c of the (a)-chain is $z \to z' = z/c_b$, whereas for the hull-functions h_b and h_d of the (b)-chain it is $z \to z' = z/c_a$.

FIG. 3. Hull-functions of the ground state for $\epsilon = 0.33$ and the particle numbers $N_a = 233$ and $N_b = 377$.

FIG. 4. Artifacts in the hull-functions for a bad choice of the particle numbers, e.g., given by $N_a = 377$ and $N_b = 610$ and the interaction strength $\epsilon = 0.33$.

FIG. 5. The interaction distance L_0 in y-direction between the upper and lower chain as function of the interaction strength ϵ. The distance L_0 is plotted in different ranges (a) from $\epsilon = 0.05, \cdots, 0.4$ and (b) from $\epsilon = 0.24, \cdots, 0.31$ (transition range).

FIG. 6. In the computation it is convenient to rescale the order parameter by $OP \to OP \cdot (\Delta z)^6$. The order parameter $OP = OP(\epsilon - \epsilon_c)$ describes the critical behaviour near the threshold ϵ_c. The graph (a) shows the behaviour of the order parameter for different particel numbers and (b) is the finite-size scaling plot of the mastered order parameter, where $OP(\epsilon)L^{\frac{\beta}{\delta}}$ is plotted versus $(\epsilon - \epsilon_c)L^{\frac{1}{\delta}}$.

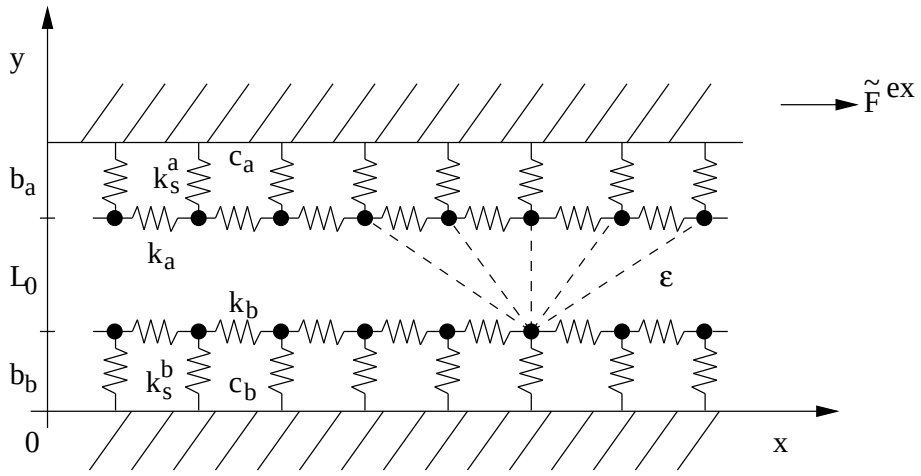

Fig. 1

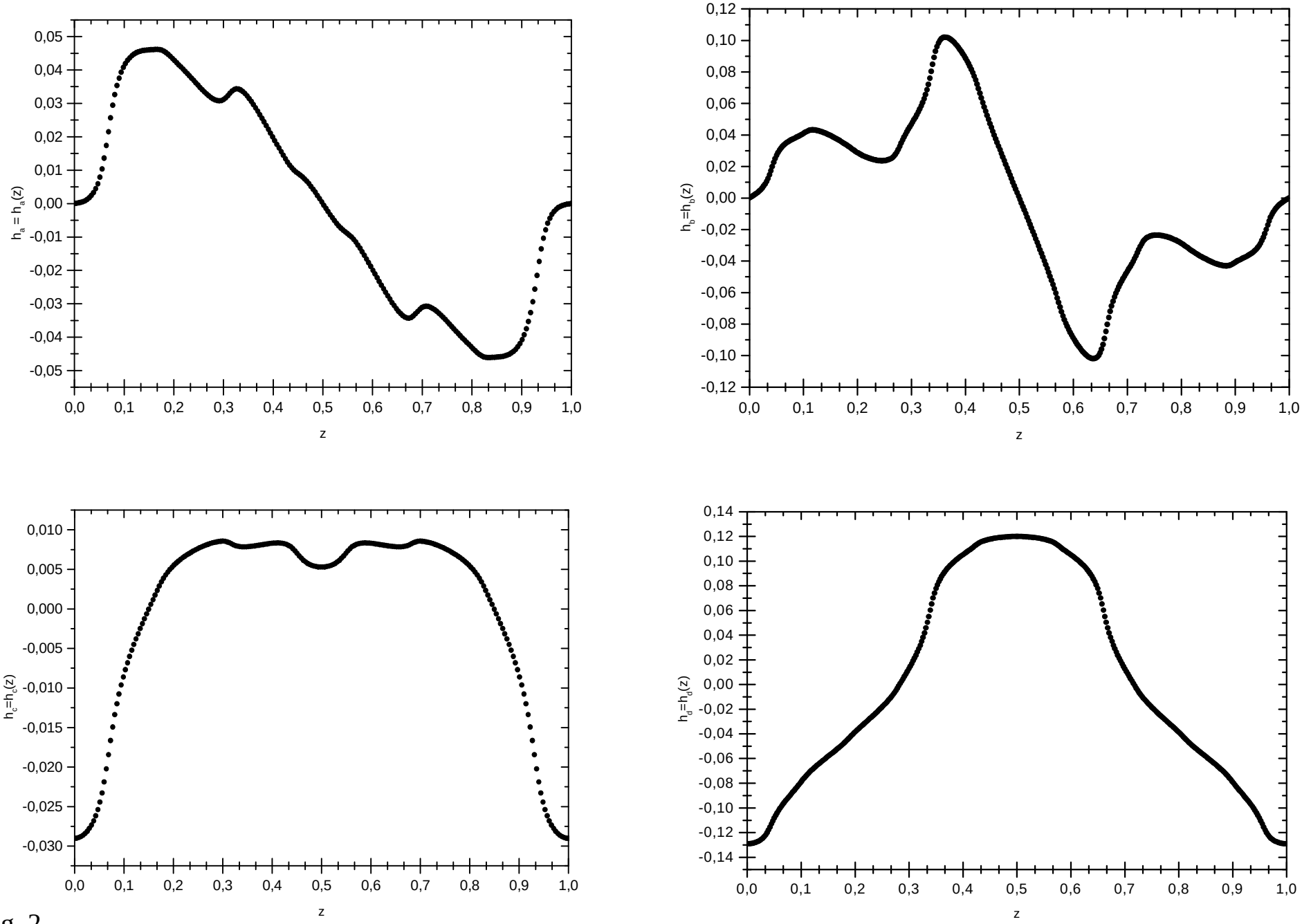
0,05
0,04
0,03
0,02
0,01
0,00
-0,01
-0,02
-0,03
-0,04
-0,05
h_a = h_a(z)
0,0 0,1 0,2 0,3 0,4 0,5 0,6 0,7 0,8 0,9 1,0
z
0,12
0,10
0,08
0,06
0,04
0,02
0,00
-0,02
-0,04
-0,06
-0,08
-0,10
-0,12
h_b=h_b(z)
0,0 0,1 0,2 0,3 0,4 0,5 0,6 0,7 0,8 0,9 1,0
z
0,010
0,005
0,000
-0,005
-0,010
-0,015
-0,020
-0,025
-0,030
h_c=h_c(z)
0,0 0,1 0,2 0,3 0,4 0,5 0,6 0,7 0,8 0,9 1,0
z
0,14
0,12
0,10
0,08
0,06
0,04
0,02
0,00
-0,02
-0,04
-0,06
-0,08
-0,10
-0,12
-0,14
h_d=h_d(z)
0,0 0,1 0,2 0,3 0,4 0,5 0,6 0,7 0,8 0,9 1,0
z

Fig. 2.

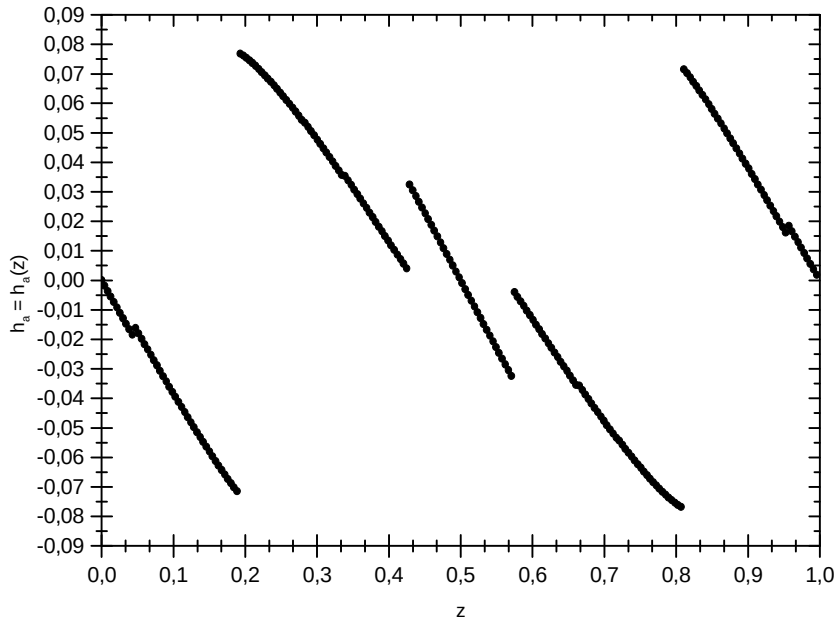
0,09
0,08
0,07
0,06
0,05
0,04
0,03
0,02
0,01
0,00
-0,01
-0,02
-0,03
-0,04
-0,05
-0,06
-0,07
-0,08
-0,09
h_a = h_a(z)
0,0
0,1
0,2
0,3
0,4
0,5
0,6
0,7
0,8
0,9
1,0
z

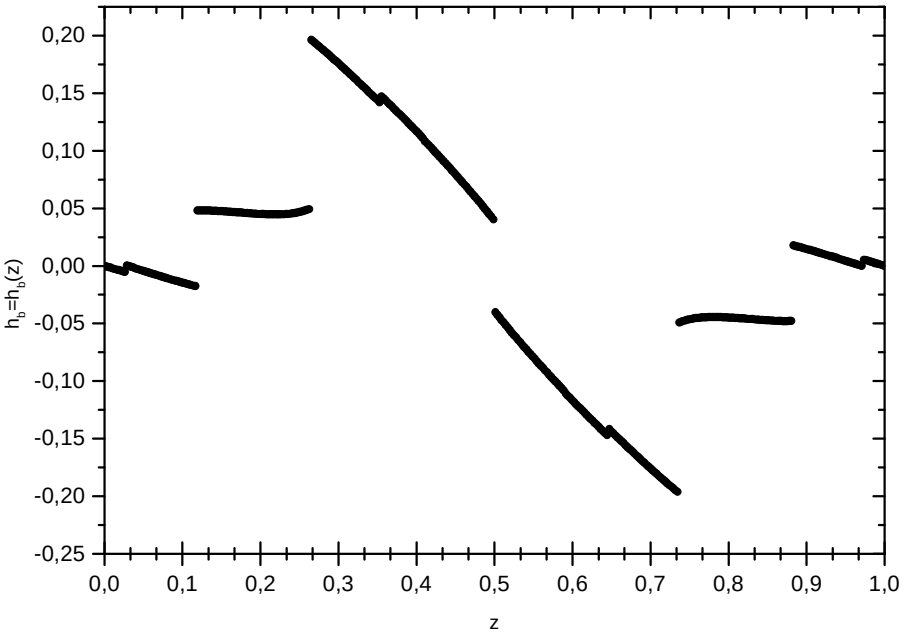
0,20
0,15
0,10
0,05
0,00
-0,05
-0,10
-0,15
-0,20
-0,25
h_b=h_b(z)
0,0
0,1
0,2
0,3
0,4
0,5
0,6
0,7
0,8
0,9
1,0
z

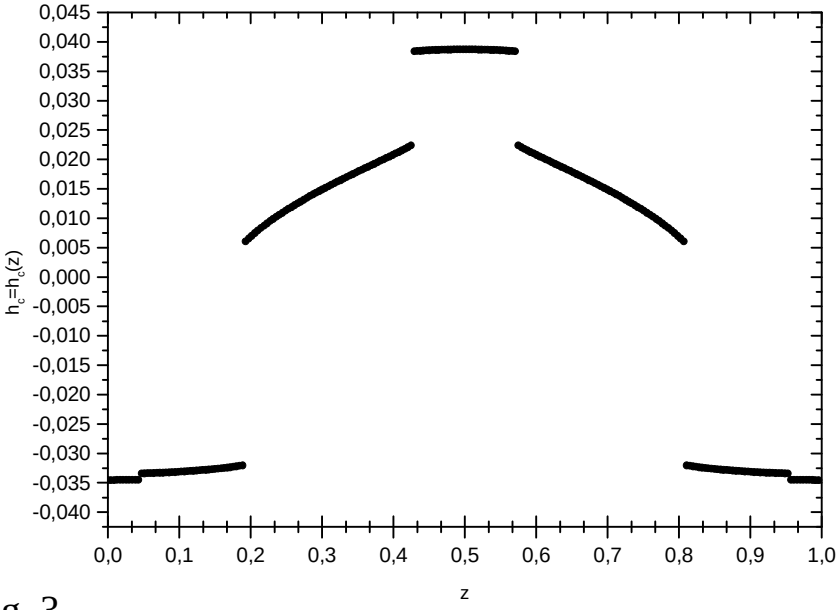
0,045
0,040
0,035
0,030
0,025
0,020
0,015
0,010
0,005
0,000
-0,005
-0,010
-0,015
-0,020
-0,025
-0,030
-0,035
-0,040
h_c=h_c(z)
0,0
0,1
0,2
0,3
0,4
0,5
0,6
0,7
0,8
0,9
1,0
z

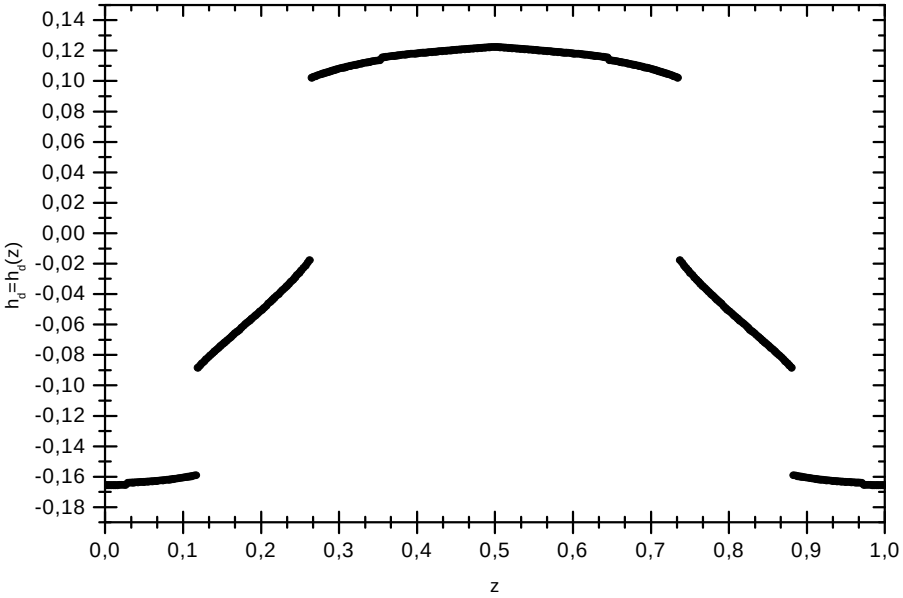
0,14
0,12
0,10
0,08
0,06
0,04
0,02
0,00
-0,02
-0,04
-0,06
-0,08
-0,10
-0,12
-0,14
-0,16
-0,18
h_d=h_d(z)
0,0
0,1
0,2
0,3
0,4
0,5
0,6
0,7
0,8
0,9
1,0
z

Fig. 3.

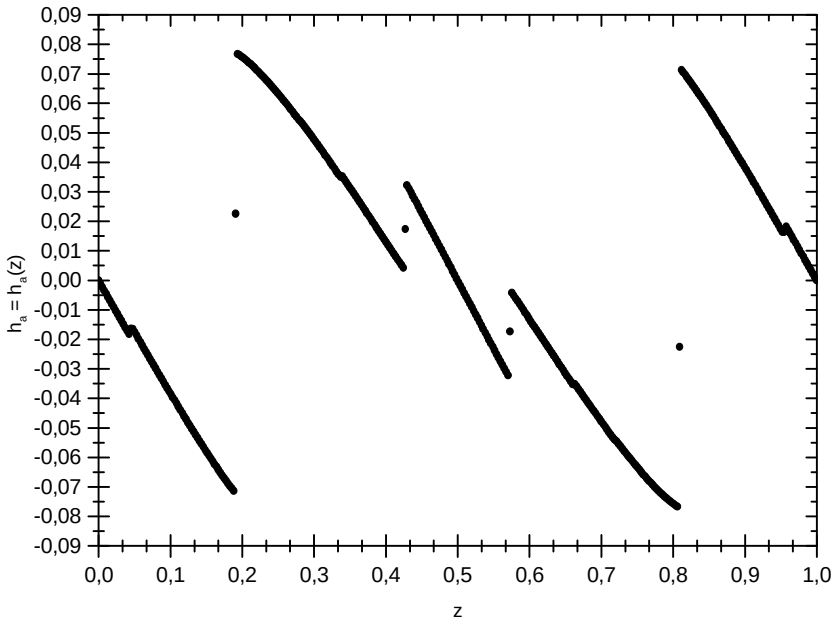
0,09
0,08
0,07
0,06
0,05
0,04
0,03
0,02
0,01
0,00
-0,01
-0,02
-0,03
-0,04
-0,05
-0,06
-0,07
-0,08
-0,09
h_a = h_a(z)
0,0
0,1
0,2
0,3
0,4
0,5
0,6
0,7
0,8
0,9
1,0
z

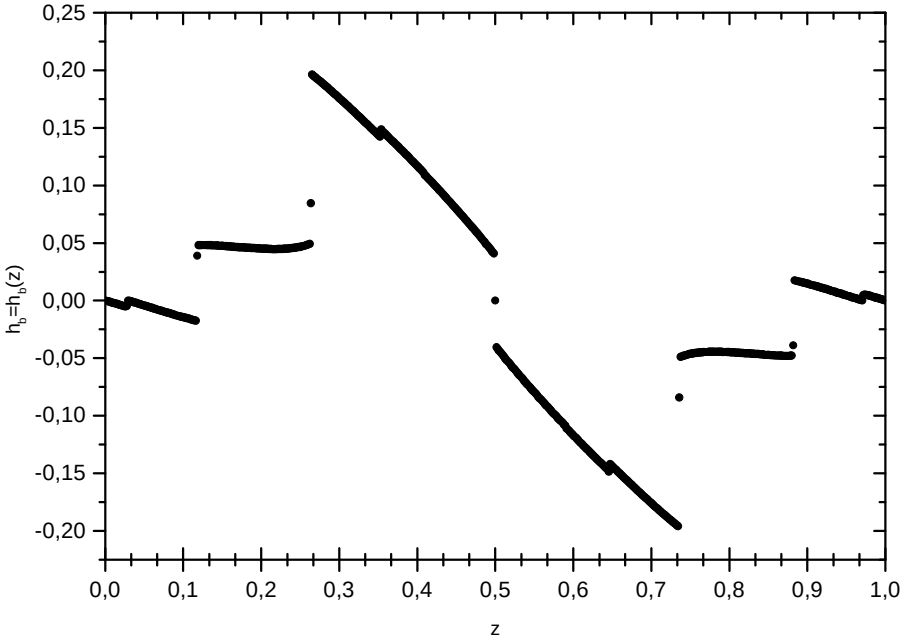
0,25
0,20
0,15
0,10
0,05
0,00
-0,05
-0,10
-0,15
-0,20
h_b=h_b(z)
0,0
0,1
0,2
0,3
0,4
0,5
0,6
0,7
0,8
0,9
1,0
z

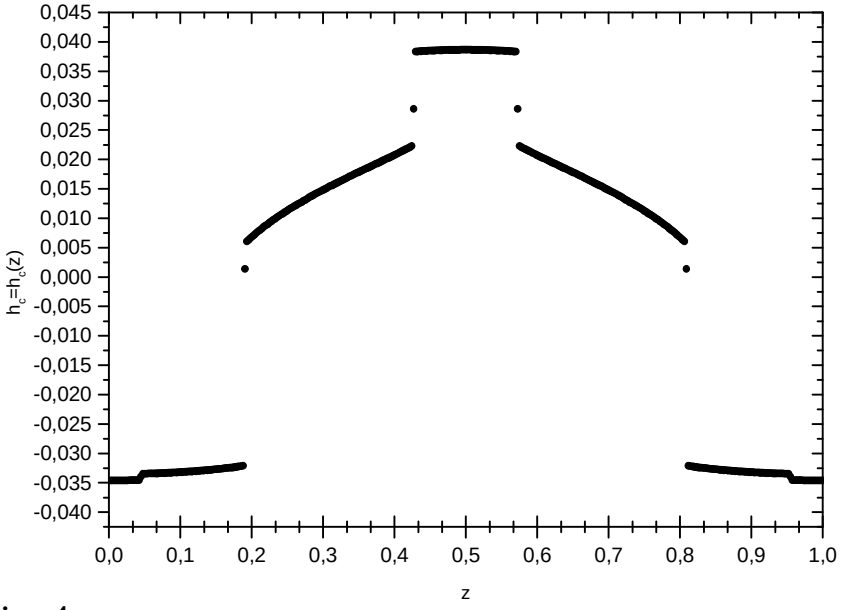
0,045
0,040
0,035
0,030
0,025
0,020
0,015
0,010
0,005
0,000
-0,005
-0,010
-0,015
-0,020
-0,025
-0,030
-0,035
-0,040
h_c=h_c(z)
0,0
0,1
0,2
0,3
0,4
0,5
0,6
0,7
0,8
0,9
1,0
z

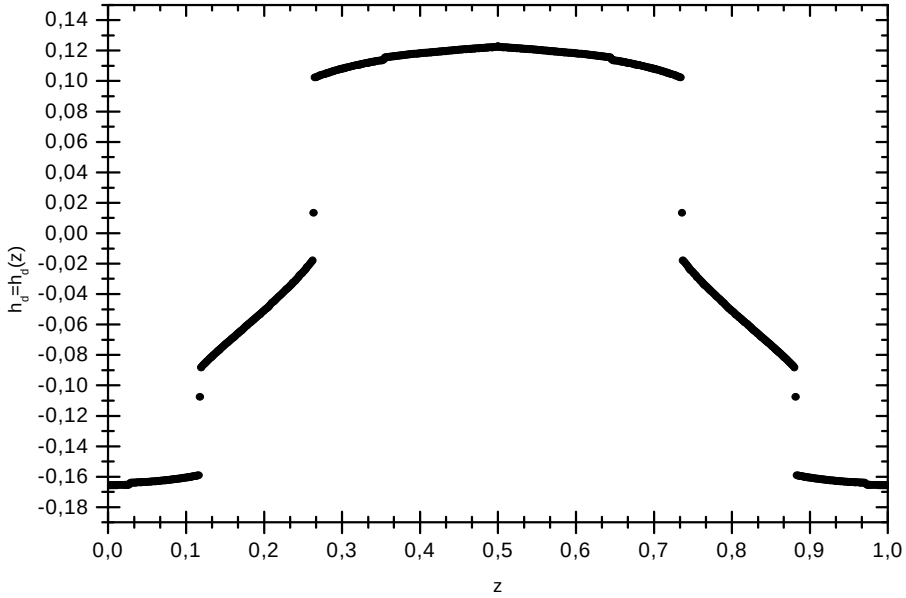
0,14
0,12
0,10
0,08
0,06
0,04
0,02
0,00
-0,02
-0,04
-0,06
-0,08
-0,10
-0,12
-0,14
-0,16
-0,18
h_d=h_d(z)
0,0
0,1
0,2
0,3
0,4
0,5
0,6
0,7
0,8
0,9
1,0
z

Fig. 4.

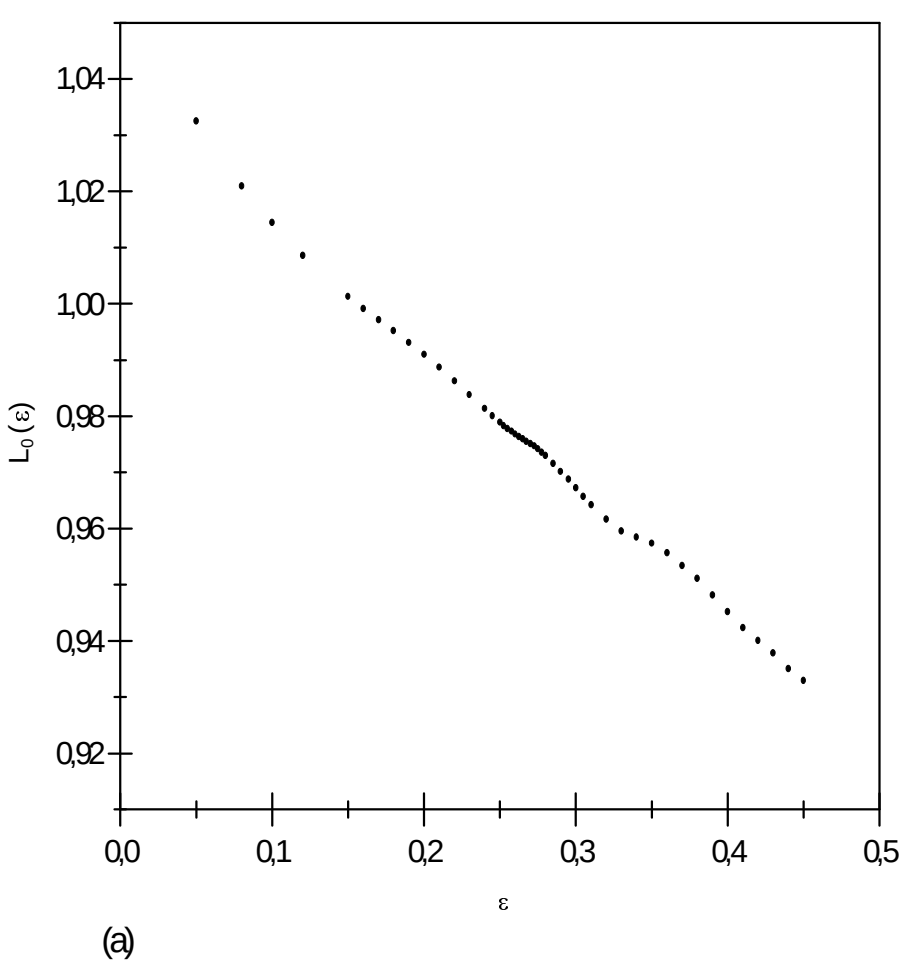
1,04
1,02
1,00
0,98
0,96
0,94
0,92
L0 (ε)
0,0
0,1
0,2
0,3
0,4
0,5
ε
(a)

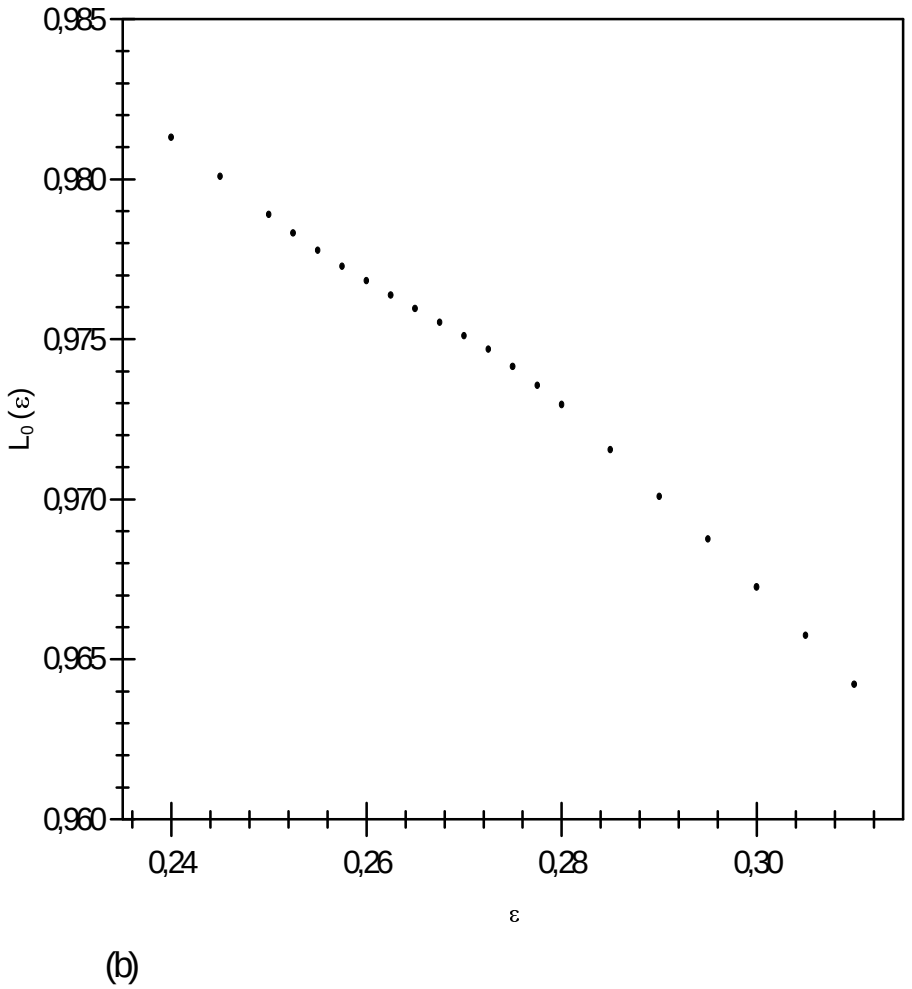
0,985
0,980
0,975
0,970
0,965
0,960
L0 (ε)
0,24
0,26
0,28
0,30
ε
(b)

Fig. 5.

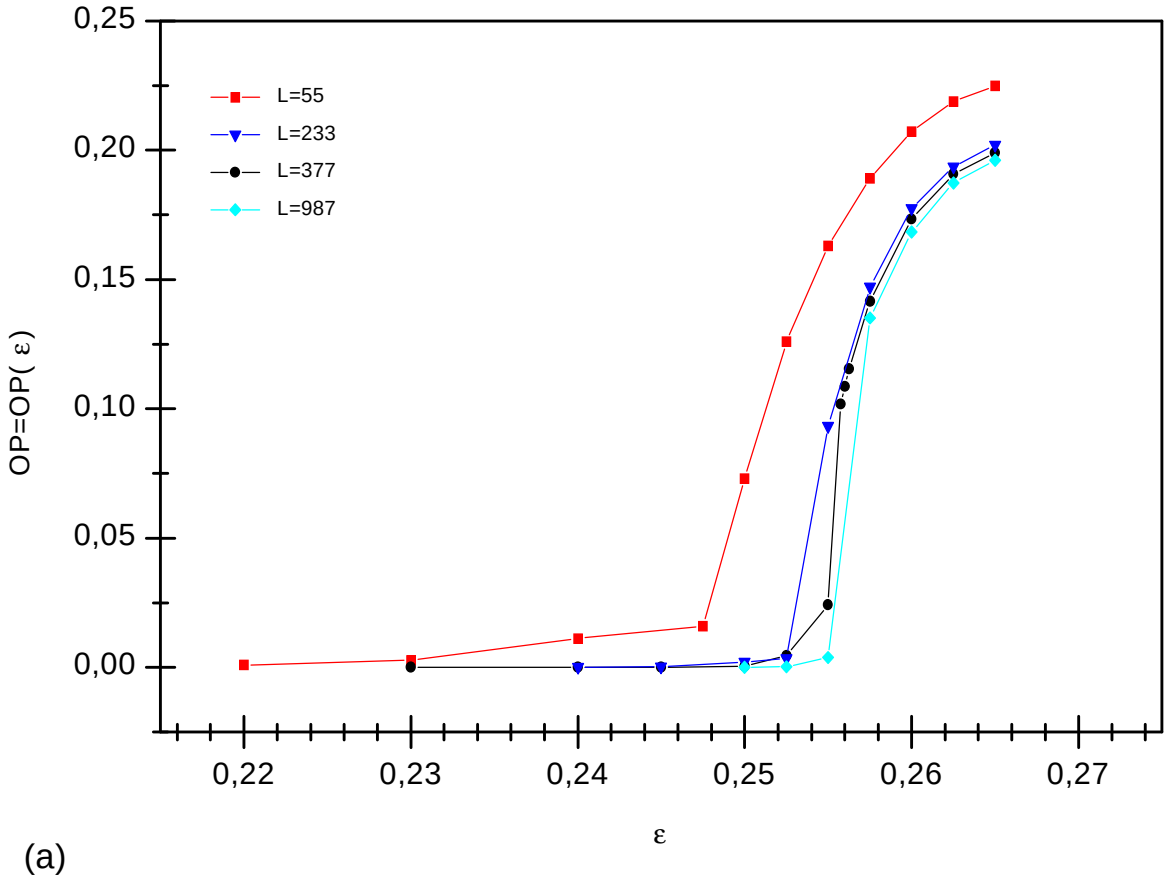
0,25
0,20
0,15
0,10
0,05
0,00
OP=OP(ε)
L=55
L=233
L=377
L=987
0,22
0,23
0,24
0,25
0,26
0,27
ε

(a)

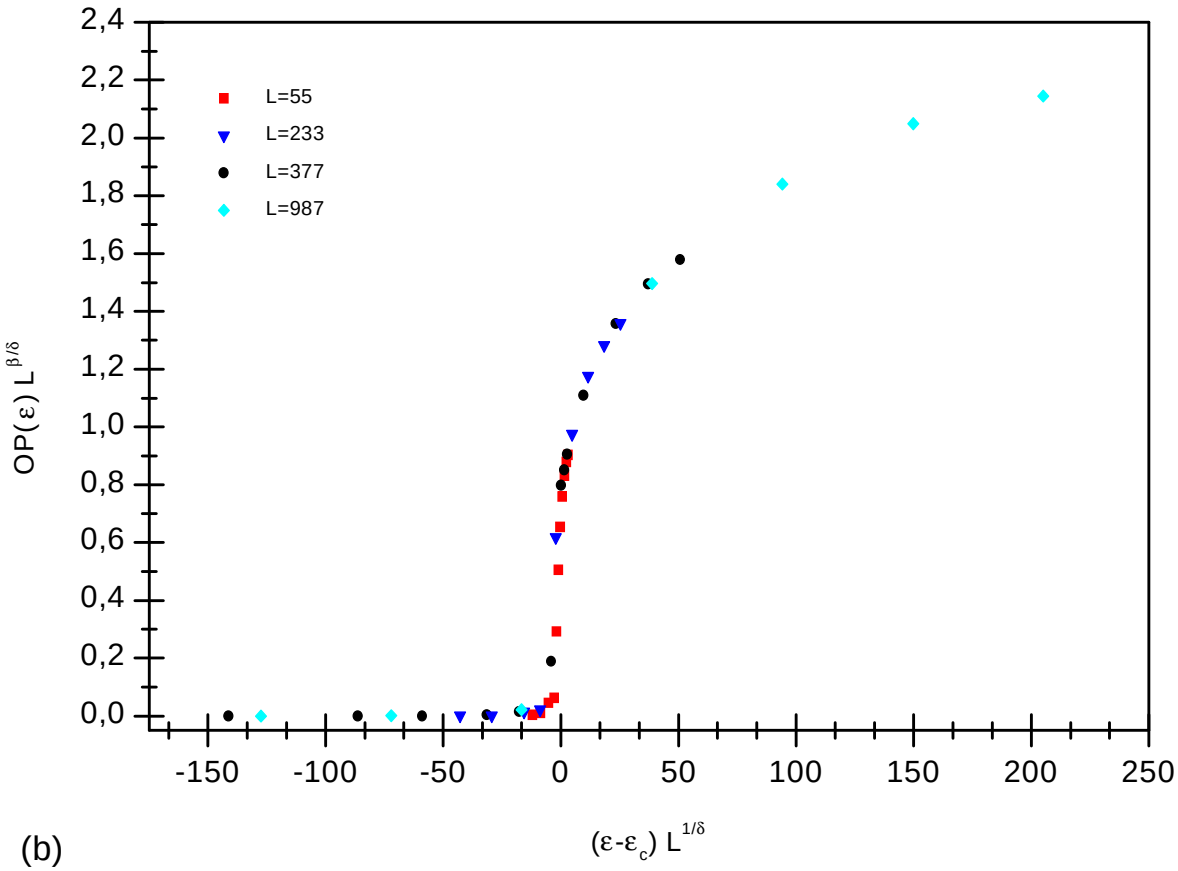
2,4
2,2
2,0
1,8
1,6
1,4
1,2
1,0
0,8
0,6
0,4
0,2
0,0
OP(ε) L^β/δ
L=55
L=233
L=377
L=987
-150
-100
-50
0
50
100
150
200
250
(ε-ε_c) L^1/δ

(b)

Fig. 6.